Synaptic activation modifies microtubules underlying transport of postsynaptic cargo

Christoph Maas[a,1], Dorthe Belgardt[a], Han Kyu Lee[a], Frank F. Heisler[a], Corinna Lappe-Siefke[a], Maria M. Magiera[b], Juliette van Dijk[b], Torben J. Hausrat[a], Carsten Janke[b], and Matthias Kneussel[a,2]

[a]Zentrum für Molekulare Neurobiologie Hamburg, Universität Hamburg, Hamburg, Germany; and [b]Centre de Recherches de Biochimie Macromoléculaire, Centre national de la recherche scientifique, Université Montpellier 1 and 2, Montpellier, France

Synaptic plasticity, the ability of synapses to change in strength, requires alterations in synaptic molecule compositions over time, and synapses undergo selective modifications on stimulation. Molecular motors operate in sorting/transport of neuronal proteins; however, the targeting mechanisms that guide and direct cargo delivery remain elusive. We addressed the impact of synaptic transmission on the regulation of intracellular microtubule (MT)-based transport. We show that increased neuronal activity, as induced through GlyR activity blockade, facilitates tubulin polyglutamylation, a posttranslational modification thought to represent a molecular traffic sign for transport. Also, GlyR activity blockade alters the binding of the MT-associated protein MAP2 to MTs. By using the kinesin (KIF5) and the postsynaptic protein gephyrin as models, we show that such changes of MT tracks are accompanied by reduced motor protein mobility and cargo delivery into neurites. Notably, the observed neurite targeting deficits are prevented on functional depletion or gene expression knockdown of neuronal polyglutamylase. Our data suggest a previously undescribed concept of synaptic transmission regulating MT-dependent cargo delivery.

activity-dependent | neuron | polyglutamylation | synapse | strychnine

Neurons change the density of postsynaptic molecules as a mechanism for changing their own excitability in response to stimuli (1–4). In dynamic processes that are maintained in equilibrium, proteins are targeted to and removed from synaptic sites (5–8). Considering the vast number of synapses present on a dendritic tree of neurons, currently, it is not well understood how new molecules are selectively targeted to individual synaptic sites on their activation. Based on the synaptic-tagging hypothesis (9), individual synapses are "tagged" by previous synaptic activity, allowing them to be selectively recognized as targets for recruitment of new molecules. However, the idea of a synaptic tag as a single molecule might be misguiding, because processes such as protein transport, local translation, or cytoskeletal reorganization could tag a synapse (9).

The majority of long-distance transport in neurites is powered by molecular motors along microtubule (MT) tracks (5, 7). Synaptic transport complexes deliver and remove neurotransmitter receptors to and from synaptic sites (5, 10), and are critically involved in memory processes in vivo (11). Currently known complexes for intracellular neurotransmitter receptor transport use scaffold proteins as adaptors to couple the motor to its vesicular cargo (6), and eventually require Ca^{2+}-dependent phosphorylation for cargo release (12). Regulation of these processes could either occur at the interface between motors and their cargoes, or alternatively, undergo regulation at the track level. Mechanisms of the latter kind include the use of different tubulin isotypes in individual MTs and/or specific posttranslational modifications of α- and β-tubulin (13).

Tubulins are prominent substrates for different types of posttranslational modifications such as detyrosination/tyrosination, acetylation, phosphorylation, polyglutamylation, and polyglycylation (13–18). Indirect evidence had previously suggested that different molecular motors and MAPs are regulated by polyglu-

tamylation, a complex polymodification of tubulin (19–21). However, functional studies on the role of these modifications remained restricted until the recent discovery of the respective modifying enzymes (15, 22). Functional evidence for the regulatory role of polyglutamylation on neuronal kinesin (KIF)-mediated transport in vivo came from knockout mice that lack a subunit of the major neuronal polyglutamylase complex (17). Besides deficiencies in neuronal development, these mice showed a clear correlation between decreased levels of tubulin polyglutamylation and abnormal targeting of individual motors in neurons (18).

Here, we investigated a new functional feedback concept, according to which synaptic activity regulates tubulin posttranslational modification, underlying intracellular transport of synaptic cargo, to determine the number of proteins available for synaptic transmission.

Results and Discussion

Activity-Dependent Gephyrin Targeting. To study activity-dependent intracellular transport, we analyzed the postsynaptic receptor clustering protein gephyrin in hippocampal neurons, cultured for 10–14 days in vitro (DIV), containing functional synapses (23, 24). Because endogenous gephyrin was already synaptic at this time, plasmids encoding autofluorescent mRFP-gephyrin were microinjected into neuronal cell bodies with the injection process representing time point 0 min. From 30 min onwards, neurons were either left untreated or treated over 8 h with the GlyR antagonist strychnine. Control conditions displayed a normal mRFP-gephyrin distribution throughout the cell with small clusters of mRFP-gephyrin signals in soma and neurites (Fig. 1A Upper), known to represent synaptic sites (10). Notably, functional GlyR blockade through strychnine instead strongly interfered with particle delivery of newly synthesized proteins into neurites. In fact, mRFP-gephyrin rather accumulated in large cell body clusters within 6–7 h, indicating severe impairment of neurite transport under receptor blockade conditions (Fig. 1A Lower). It should be noted that the fusion proteins analyzed here, represented newly expressed polypeptides from cDNA constructs that had been microinjected just 8.5 h before quantitative analysis, with initial expression signals detectable after 6 to 7 h. Therefore, the observed effects represent changes in the anterograde transport direction. Quantitative evaluation of signal numbers, sizes, and intensities revealed highly
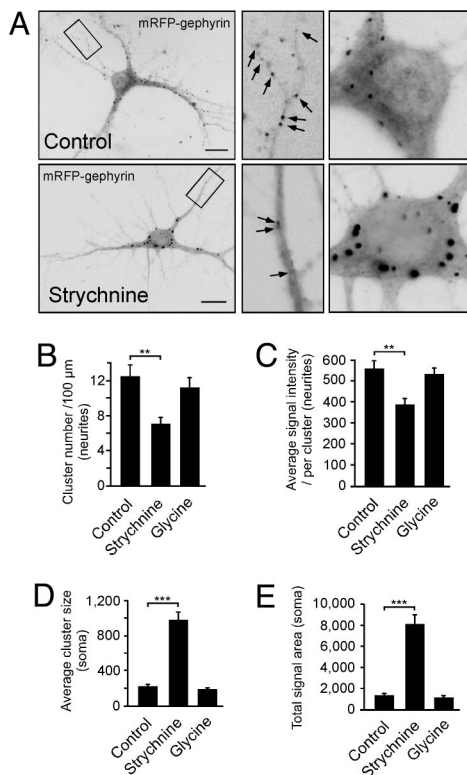
Fig. 1. Activity changes alter gephyrin delivery into neurites. (*A*) Cultured neurons microinjected with mRFP-gephyrin cDNA (time point, 0 min), cultured for 8 h with (*Lower*) or without (*Upper*) strychnine. Quantitative analysis of fluorescent mRFP-gephyrin signals at time point 8.5 h. Note that mRFP-gephyrin expression requires 6–7 h; detected signals represent newly synthesized protein. (*B–E*) Quantitative analysis of gephyrin signal numbers, sizes, and intensities in neurites and somata. Neurons were either treated with solvent (control), strychnine, or glycine [12–16 neurons, each; 3–4 experiments (arbitrary units)]. For original values, see *SI Experimental Procedures*. Data: means ± SEM. (Scale bar, 25 μm.)

significant changes in neurites and somata on GlyR blockade, as compared with untreated control conditions (Fig. 1 *B–E*), indicating that neurite targeting of the postsynaptic GlyR clustering protein gephyrin follows activity-dependent processes that are sensitive to changes in GlyR-mediated synaptic transmission. Notably, AMPA receptor (AMPAR) activation through AMPA led to similar results as seen on strychnine-mediated GlyR blockade (Fig. S1 *A–E*), suggesting that the observed transport deficits were not restricted to changes in glycinergic transmission, but rather because of a general increase in neuronal activity. In coherence with this view, blockade of AMPARs through the antagonist 6,7-dinitroquinoxaline-2,3-dione (DNQX) did not induce deficits in mRFP-gephyrin delivery to neurites, and led to a cluster distribution (Fig. S1 *A–E*), similar as previously observed under control conditions (Fig. 1). Accordingly, also the application of glycine, known to increase the activity of inhibitory GlyRs, did not interfere with mRFP-gephyrin particle delivery into neurites (Fig. 1 *B–E*). Therefore, we conclude that neuronal depolarization and/or increased activity represents a negative signal for particle transport in this system.

KIF5-Gephyrin-GlyR Complex for Anterograde Transport. To test whether gephyrin might physically bind to an anterograde-directed MT motor of the KIF family that could potentially mediate transport to the neuronal periphery, we applied coimmunoprecipitation on $100,000 \times g$ (P3) vesicle-enriched intracellular fractions, derived from postnatal day (P)10 rat brain lysate. These experi-

ments revealed that conventional KIF (KIF5) interacts with gephyrin in vitro (Fig. 2*A* and Fig. S2 *A and B*). Notably, also GlyRs were subject to coprecipitation, and the use of antibodies, specific for either GlyR, gephyrin, or KIF5, coprecipitated the other 2 proteins. These results were specific, because neither an unrelated receptor subunit (NMDAR2B), nor an unrelated KIF (KIF1B) were subject to coprecipitation (Fig. 2*B*).

To prove KIF5 specificity through loss-of-function, we then microinjected mRFP-gephyrin cDNA (25), together with KIF5-specific antibodies (26, 27). On microinjection, the respective neurons displayed a healthy morphology and the typical widespread mRFP-gephyrin distribution after 8 h of expression (Fig. 2*C Upper*). In contrast, and similar as seen on the depolymerization of MTs (Fig. S3 *A–D*), injection of a mixture of 2 independent pan-KIF5 antibodies, known to efficiently block KIF5 function (26, 27), severely inhibited mRFP-gephyrin targeting into neurites (Fig. 2*C Lower*). Similar as seen in the presence of strychnine, quantitative evaluation again revealed highly significant changes in cluster numbers, sizes, and signal intensities in both the soma and neurites (Fig. 2 *D–G*). These changes were not observed on injection of a KIF1B-specific antibody (Fig. 2 *D–G*; compare with Fig. 2*B*), indicating that motor function of KIF5 is indeed essential and specific to drive newly synthesized mRFP-gephyrin into neurite processes. In a further complementary loss-of-function experiment, we interfered with gephyrin rather than KIF5 motor functions, by using a previously established antisense oligonucleotide-based protocol to efficiently deplete gephyrin gene expression (28). According to previous reports, antisense oligonucleotide treatment of cultured neurons from DIV2 until DIV12 reduced gephyrin expression levels to ≈7%, as compared with sense controls (Fig. 2 *H* and *I*). This result enabled us to combine down-regulation of gephyrin expression with a surface membrane biotinylation experiment, to quantitatively evaluate the amount of GlyR plasma membrane levels under antisense-oligonucleotide conditions. Notably, gephyrin knockdown caused a highly significant reduction of GlyR surface localization to relative signal intensities of ≈40% compared with control levels (Fig. 2 *J* and *K*). Together, these data confirm that gephyrin represents a critical mediator for GlyR plasma membrane delivery. Given that GlyR activity-blockade in turn affects gephyrin transport into the neuronal periphery (Fig. 1), a functional feedback loop might exist that mediates cross-talk between the synaptic surface membrane and the intracellular transport machinery. Because gephyrin binds directly to both the receptor (29, 30) and the kinesin motor (Fig. S2*B*), a putative MT-dependent transport complex, with gephyrin representing the motor-cargo adaptor, is likely to undergo intracellular regulation.

Activity-Dependent Polyglutamylation of Tubulin. To assess whether GlyR activity blockade could directly affect MTs, we analyzed the known posttranslational modifications of tubulin under control or strychnine-mediated conditions. DIV11–14 cultured neurons were either untreated or treated with 1 μM strychnine for 8 h, followed by the preparation of cytoskeletal fractions. Quantitative Western blot analysis, using 2 independent antibodies (B3 and GT335) specific to tubulin polyglutamylation, revealed a significant increase of polyglutamylation levels in the presence of GlyR blockade, as compared with control conditions and α-tubulin detections (Fig. 3 *A–D*). In contrast, the amounts of other posttranslational modifications of tubulin, detyrosination and acetylation (14), remained unaltered (Fig. 3 *E* and *F*). These observations suggested that changes in synapse activity specifically regulate polyglutamylation processes, and that the respective polyglutamylase(s) might act downstream of an activity-dependent signaling cascade.

Polyglutamylation of tubulin might have the potential to regulate the binding of MT-associated proteins (MAPs) to MTs, and MAP2 has been shown to preferentially bind tubulin with glutamate side chains of ≈3 glutamyl units in blot overlay assays (19). Therefore, we asked whether strychnine treatment resulted in an altered

Fig. 2. KIF5, gephyrin, and GlyR associate in an anterograde-directed transport complex. (*A* and *B*) Coimmunoprecipitation experiment. Precipitation (vertical) and detection (horizontal) with GlyR, gephyrin, or KIF5 antibodies are shown. Controls: NMDAR2B and KIF1B detection. (*C*) DIV10–14 neurons microinjected with either IgG, pan-KIF5, or KIF1B antibodies, respectively, together with EGFP and mRFP-gephyrin expression constructs. Analysis done after 8 h. (Scale bar, 15 μm.) (*D*–*G*) Quantitative analysis of fluorescent mRFP-gephyrin signal numbers, sizes, and intensities [5–15 neurons, each; 3–4 experiments (arbitrary units)]. For original values, see *SI Experimental Procedures*. Data: means ± SEM. (*H* and *I*) Gephyrin knockdown. Antisense, but not sense, oligonucleotides (DIV2–12) reduce gephyrin expression to ≈7%, (gephyrin/actin signal ratios, relative signal intensities in %). (*I*) Gephyrin total expression. Sense, set to 100% (*n* = 3); antisense, 6.55 ± 3.10% (*n* = 3). (*J* and *K*) Surface biotinylation experiment. GlyR surface membrane delivery on gephyrin knockdown is shown. Antisense oligonucleotide-mediated gephyrin knockdown reduces GlyR surface membrane levels to ≈40% ($P < 0.01$) (GlyR/Cadherin signal ratios, relative signal intensities in %). (*K*) GlyR surface membrane expression. Sense, set to 100% (*n* = 3); antisense, 40.71 ± 11.60 (*n* = 3). Data: means ± SD.

binding of MAPs to MTs, in particular because MAP2 has also been implicated in activity-dependent processes. In fact, MAP2 binding to MTs in living cells depends on its phosphorylation state (31), with MAP2 phosphorylation in turn critically depending on activity changes in the neuron (32). Therefore, we quantitatively analyzed the amount of MAP2 binding to MTs under control and strychnine-mediated conditions, by using cytoskeletal fractions from cultured neurons after Triton X-100 extraction. Western blot analysis indeed revealed strong MAP2 accumulation in the cytoskeletal fractions on GlyR blockade, as compared with untreated neurons and an α-tubulin loading control (Fig. 3 *G* and *I*). In contrast, levels of the actin binding protein myosin V, normalized to a loading control, remained completely unaltered under identical conditions (Fig. 3 *H* and *I*), indicating specificity of activity-dependent MAP2 binding to MTs.

Nine different polyglutamylase enzymes are known in mammals (15). However, neuronal polyglutamylase activity is mainly associated with only one of them: a multiprotein complex referred to as neuronal polyglutamylase. This complex consists of 5 subunits, called PGs1-5 and immunodepletion of the complex from brain tissue extracts led to the depletion of ≥80% of polyglutamylase activity (22). If tubulin polyglutamylation acted as a negative signal for gephyrin transport into neurites, inactivation of polyglutamylating enzymes should reverse or prevent the identified gephyrin targeting deficits on GlyR activity blockade (Fig. 1). To deplete the enzymatic activity of the neuronal polyglutamylase, we microinjected mRFP-gephyrin expression constructs together with a mixture of PGs1 and PGs2-specific antibodies into cultured neurons, and analyzed the arrival of newly synthesized mRFP-gephyrin puncta in neurites. An in vitro activity assay confirmed that both antibodies are suitable to deplete the enzymatic function of neuronal polyglutamylase in extracts of these cells (Fig. S4*A*). Neuronal injection of either unspecific IgG antibodies (control) or anti-PGs1/2 did not per se influence delivery of mRFP-gephyrin into the distal dendritic tree (Fig. S4*B*). However, anti-PGs1/2, but not IgG injection in the presence of strychnine, efficiently prevented the

Fig. 3. Activity-dependent polyglutamylation of MTs. (*A–F*) Quantitative cytoskeletal fraction analysis of neurons cultured with or without strychnine (α-tubulin, loading control). Control values are set to 1 (relative intensities of signal/tubulin signal ratios). B3, strychnine: 2.60 ± 0.57 (*n* = 8 experiments); GT335, strychnine: 2.03 ± 0.51 (*n* = 11 experiments); acetylated tubulin, strychnine: 1.14 ± 0.16 (*n* = 3 experiments); tyrosine tubulin, strychnine: 1.12 ± 0.15 (*n* = 3 experiments). (*G–I*) GlyR blockade increases MAP2 binding to MTs. (*G*) Cytokeletal fraction analysis of neurons with or without strychnine (detection, anti-MAP2; α-tubulin detection, loading control). (*H*) Control experiment detecting an unrelated cytoskeleton-associated protein (myosinV) (actin detection, loading control). (*I*) Quantitative analysis of *G* and *H*. Data: mean ± SEM. Control values are set to 1 (relative intensities of signal/actin signal ratios). MAP2, strychnine: 4.24 ± 0.35 (*n* = 3 experiments); Myosin V, strychnine: 1.01 ± 0.14 (*n* = 3 experiments). (*J–N*) Cultured neurons microinjected with mRFP-gephyrin cDNA in the presence of strychnine and either unspecifc IgG or a mixture of anti-PGs1/anti-PGs2 antibodies (injection, 0 min; signal analysis at 8.5 h). The combinatorial use of strychnine and anti-PGS1/2 injection (*Lower*) prevents gephyrin transport inhibition (*Upper*), leading to normal transport into neurites. (*K–N*) Quantitative analysis of signal numbers, sizes, and intensities in neurites and somata [12 neurons, each; 3–4 experiments (arbitrary units)]. For original values, see *SI Experimental Procedures*. (*O–R*) Quantitative Western blot analysis of neurons infected with either a control lentivirus or an shRNA-PGs1 lentivirus (α-tubulin, loading control). Control values are set to 1 (relative intensities of signal/tubulin signal ratios). (*O* and *P*) PGs1 detection, 0.44 ± 0.21 (*n* = 3 experiments). (*Q* and *R*) Polyglutamylation (B3) detection, 0.46 ± 0.16 (*n* = 4 experiments). (*S–V*) Lentivirus mediated delivery of shRNA for PGs1 knockdown also prevents the strychnine-mediated blockade of mRFP-gephyrin transport into neurites. Quantitative analysis of signal numbers, sizes, and intensities in neurites and somata are shown [11–15 neurons, each; 3–4 experiments (arbitrary units)]. For original values, see *SI Experimental Procedures*. Data: means ± SEM.

previously observed targeting blockade of mRFP-gephyrin toward the neurite periphery (Fig. 3*J*; compare with Fig. 1). Consequently, these effects led to highly significant changes in signal numbers, sizes, and intensities throughout both neurites and somata (Fig. 3 *K–N*). These results were specific, because prevention of the mRFP-gephyrin transport blockade on strychnine treatment could also be observed in a second independent rescue approach. Notably, lentivirus infection of neurons, leading to shRNA-mediated knockdown of PGs1 gene expression (Fig. 3 *O* and *P*), decreased polyglutamylation levels (Fig. 3 *Q* and *R*), and consequently mimicked the loss-of-function results on PGs1/2 antibody injection (Fig. 3 *S–V*). Therefore, we conclude that polyglutamylation of neuronal MTs, mediated through the previously identified neuronal polyglutamylase complex (15), regulates GlyR-gephyrin neurite targeting in an activity-dependent manner.

Specific Rather than General Mobility Changes on GlyR Activity Blockade. Polyglutamylation is known to regulate MAP2 binding (19), which could in turn interfere with motor protein mobility (33, 34). Because of the above results, we further asked whether polyglutamylation acted in general as a negative signal for KIF5-mediated transport in neurons. Application of neuronal live cell imaging revealed that GlyR blockade significantly reduced KIF5 particle mobility over time, although KIF5, known to transport multiple cargoes, remains mobile (Fig. 4*A*). Analysis at the cargo adaptor level showed that mRFP-gephyrin particle mobility was also significantly reduced after drug application (ada) of strychnine over 4 h (Fig. 4*B*; Movie S1 and Movie S2). These changes were specific, because glycine application did not alter mRFP-gephyrin particle mobility (Fig. S4*C*). Notably, KIF5-mediated GRIP1 particle movement, the latter protein representing the cargo adaptor for AMPA-receptor synaptic transport, driven by the same motor protein, remained completely unaffected in the presence of strychnine (Fig. 4*C*; Movie S3 and Movie S4). This result suggests that activity-dependent signals modify the MT-level to alter transport of specific motor-cargo complexes, without affecting motor transport in general. Consequently, individual cargo adaptors, however, not primarily the actual motor protein itself, might represent the crucial factors in sensing regulatory signals at the track level.

Local instead of global increases in synaptic activity that induce negative transport signals in a restricted location, would be most suitable to target and direct specific cargo complexes. Consequently, whether the described MT modifications would be preferentially induced in one, but not the other arm of a dendrite (Fig. 4*D*), the described signals could modify transport toward a specific neurite branch or interfere with cargo-flux toward a local subregion. Alternative signals that might act downstream or in parallel interfere with KIF17-mediated cargo transport. On NMDA receptor-mediated Ca^{2+} influx, CaMKII is activated and in turn leads to phosphorylation and a local dissociation of the actual motor-cargo complex (12).

The data in the present study suggest that the initiation of MT modifications (polyglutamylation, MAP binding to MTs) depend on a general increase in neuronal depolarization and/or activity, as they can be observed either by blocking inhibitory GlyRs, or by activating excitatory AMPARs. Therefore, the respective enzyme (neuronal polyglutamylase) might be a component of an activity-dependent signaling cascade.

Tubulin polyglutamylation is the critical signal in regulating gephyrin delivery to distal dendrites, because functional depletion of neuronal polyglutamylase prevents the observed transport deficits (Fig. 3). Polyglutamylation has been shown to regulate MAP interactions with MTs (19). Consistent with strychnine application acting as a negative signal for KIF5 mobility (Fig. 4*A*), MAP2 is known to negatively influence KIF transport (33, 34). Therefore, an increased binding of MAP2 to MTs might be a suitable mechanism to regulate motor protein mobility. However, whether polyglutamylation acts exclusively upstream of MAP2 binding to MTs, or
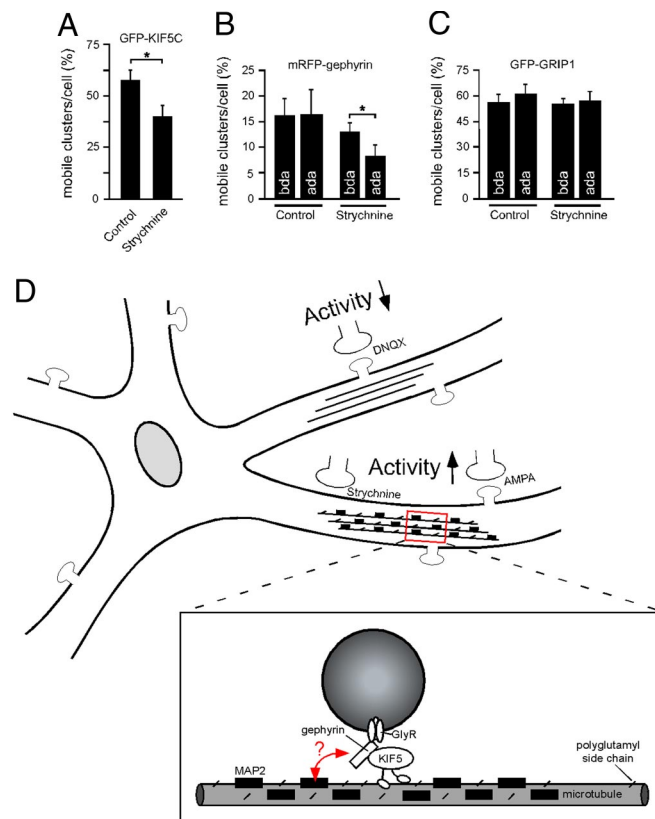

Fig. 4. Quantitative analysis of particle mobilities. (*A–C*) Neuronal live cell imaging in the absence or presence of strychnine. Data: means ± SEM. (*A*) GFP-KIF5C (*n* = 3 experiments, >800 particles). Control (solvent): 57.39 ± 5.02, *n* = 20 neurons; Strychnine: 39.95 ± 5.89, *n* = 21 neurons. (*B*) Monomeric RFP-gephyrin (*n* = 3 experiments, >450 particles). Control (solvent), *n* = 8 neurons; bda, 16.08 ± 3.18; Control (solvent), ada: 16.45 ± 4.73; Strychnine, *n* = 18 neurons, bda: 12.92 ± 1.80; Strychnine, ada: 8.21 ± 2.10. (*C*) GFP-GRIP1 (*n* = 3 experiments, >1,700 particles). Control (solvent), *n* = 9 neurons, bda: 57.19 ± 5.16; Control (solvent), ada: 61.70 ± 5.76; Strychnine, *n* = 10 neurons, bda: 55.83 ± 3.73; Strychnine, ada: 57.60 ± 5.61. (*D*) Model of MT track changes through polyglutamylation and MAP binding on altered neuronal activity. Increased activity, as induced through GlyR blockade (strychnine; Fig. 1) or AMPAR activation (AMPA; Fig. S1) interferes with gephyrin delivery into distal neurites. This effect is not observed on neuronal activity reduction through AMPAR blockade (DNQX; Fig. S1), and is prevented through functional depletion of neuronal polyglutamylase (Fig. 3 *J–V*). Increased activity through GlyR blockade facilitates tubulin polyglutamylation and MAP2 binding to MTs (strychnine; see Fig. 3 *A*, *B*, and *G*). Although it is unclear which modification is dominant, both represent negative signals for cargo delivery. Accordingly, strychnine treatment interferes with KIF5 mobility on the induction of the aforementioned track modifications (*A*). Notably, KIF5-mediated transport of gephyrin is significantly reduced under strychnine conditions, whereas KIF5-mediated transport of GRIP1 remains unaltered (*B* and *C*). These data suggest that the specificity of transport regulation is mediated through the individual cargo adaptor (red arrow), acting as a sensor of the MT surface [gephyrin connects KIF5 with GlyR (Fig. 2 and Fig. S3); GRIP1 connects KIF5 with AMPAR (35)]. Such a role of cargo adaptors is consistent with their previously identified role in determining cargo directionality to either axons or dendrites (35).

whether both modifications could per se interfere with motor protein mobility, currently remains elusive.

Notably, specificity of this regulatory system is given by the use of the individual cargo adaptor that connects motors and receptors. KIF5-mediated transport of gephyrin is significantly reduced under strychnine conditions (Fig. 4*B*), whereas KIF5-mediated transport of GRIP1 remains unaltered (Fig. 4*C*). Because both gephyrin and GRIP1 bind to the same motor [gephyrin connects KIF5 with GlyR (Fig. 2 and Fig. S2); GRIP1 connects KIF5 with AMPAR (35)], this

NEUROSCIENCE

observation suggests that cargo adaptors might act as sensors of the MT surface that enable the system to distinguish individual patterns of track modifications (Fig. 4*D*). Such interpretations on the role of cargo adaptors is consistent with a previous study, which showed that cargo adaptors (GRIP1 vs. JSAP) determine cargo directionality and encode whether cargoes are sorted to axons or dendrites, respectively (35).

In summary, our data provide evidence for activity-dependent cross-talk between synaptic transmission and tubulin posttranslational modifications underlying intracellular MT transport. They suggest that the novel concept that transport regulation not only occurs at the level of the motor-cargo complex, but in addition involves the level of the transport track.

Experimental Procedures

Cell Culture/Microinjection. Cell culture and microinjection were performed as described (25). For additional details refer to *SI Experimental Procedures*.

Preparation of Cytoskeletal Fractions. For preparation of the cytoskeleton cultured hippocampal neurons were treated with 3 μM 1-β-D-arabinofuranosylcytosine to avoid astrocyte proliferation. Preparation was performed as previously described (36). Living neuronal cultures grown in 24 well plates were treated with 1 μM strychnine (Sigma) at 11–13 DIV for 8 h at 37 °C. After incubation cells were washed with prewarmed MT-stabilizing buffer (0.13 M Hepes, pH 6.9/2 mM MgCl$_2$/10 mM EGTA), extracted in the same buffer with 1% Triton X-100 for 2 min at 37 °C, and a second time washed with prewarmed MT-stabilizing buffer. The Triton X-100-insoluble cytoskeletal fraction on the coverslips was harvested in SDS-reducing sample buffer using a cell scraper, boiled, and examined by Western blot analysis.

Coimmunoprecipitation. Coimmunoprecipitation was performed as described (10). For additional details, see *SI Experimental Procedures*.

Antisense Oligonucleotide Knockdown/Surface Biotinylation. Primary hippocampal neurons (10, 23, 37) were treated with phosphorothioate-modified sense or antisense oligonucleotides covering the translation start codon (nucleotide position 261–285) of the gephyrin cDNA sequence from DIV2 until DIV12 with daily delivery of oligonucleotides as described (28, 38). At DIV12, the culture medium was supplemented with 1 mM biotinamidohexanoic acid 3-sulfo-N-hydroxysuccinimid-ester sodium salt (Sigma) and incubated for 20 min at 4 °C to label surface proteins with biotin. Remaining biotin reagent was quenched by incubation with 100 mM glycine in Hepes buffer (twice for 20 min at 4 °C). Cells were then washed with icecold PBS and lysed in PBS containing 1% Triton X-100 (Merck) and protease inhibitor mixture (Roche). After a 30-min incubation period on ice followed by brief centrifugation at 5,000 $\times$ *g* for 5 min at 4 °C, the supernatant was added to 20 μL of prewashed magnetic MyOne streptavidin C1 beads (Dynal), followed by incubation at 4 °C for 3 h on a rotating wheel. Beads were washed twice with IP washing buffer (50 mM Tris/150 mM NaCl/5 mM MgCl$_2$, pH 7.5) containing 0.5% Triton X-100, collected, and boiled in SDS sample buffer.

Live Cell Imaging. Live cell imaging (time-lapse video microscopy) was performed with an inverted fluorescent microscope Zeiss Axiovert 200M (Zeiss) combined with a Sony CCD-Kamera (Visitron). After imaging of mRFP-gephyrin- or GFP-GRIP1-expressing neurons in the absence of drugs (bda, before drug application), either solvent, 1 μM strychnine or 250 μM glycine were applied, respectively. Cells were incubated for another 4–5 h in the presence of these drugs before additional movies of the identical cells were aquired. For GFP-KIF5C mobility analysis, neurons were either treated with solvent or 1 μM Strychnine, respectively. Movies were taken 7–9 h ada. All images were taken at 5- to 10-s intervals over 300 s, each. Cells at the microscope stage were temperature controlled and kept in Hepes-buffer.

1. Kennedy MJ, Ehlers MD (2006) Organelles and trafficking machinery for postsynaptic plasticity. *Annu Rev Neurosci* 29:325–362.
2. Malenka RC, Bear MF (2004) LTP and LTD: An embarrassment of riches. *Neuron* 44:5–21.
3. Choquet D, Triller A (2003) The role of receptor diffusion in the organization of the postsynaptic membrane. *Nat Rev Neurosci* 4:251–265.
4. Kneussel M, Betz H (2000) Clustering of inhibitory neurotransmitter receptors at developing postsynaptic sites: The membrane activation model. *Trends Neurosci* 23:429–435.
5. Hirokawa N, Takemura R (2005) Molecular motors and mechanisms of directional transport in neurons. *Nat Rev Neurosci* 6:201–214.
6. Kneussel M (2005) Postsynaptic scaffold proteins at non-synaptic sites. *EMBO Rep* 6:22–27.
7. Caviston JP, Holzbaur EL (2006) Microtubule motors at the intersection of trafficking and transport. *Trends Cell Biol* 16:530–537.
8. Ziv NE, Garner CC (2004) Cellular and molecular mechanisms of presynaptic assembly. *Nat Rev Neurosci* 5:385–399.
9. Martin KC, Kosik KS (2002) Synaptic tagging – who's it? *Nat Rev Neurosci* 3:813–820.
10. Maas C, et al. (2006) Neuronal cotransport of glycine receptor and the scaffold protein gephyrin. *J Cell Biol* 172:441–451.
11. Wong RW, Setou M, Teng J, Takei Y, Hirokawa N (2002) Overexpression of motor protein KIF17 enhances spatial and working memory in transgenic mice. *Proc Natl Acad Sci USA* 99:14500–14505.
12. Guillaud L, Wong R, Hirokawa N (2008) Disruption of KIF17-Mint1 interaction by CaMKII-dependent phosphorylation: A molecular model of kinesin-cargo release. *Nat Cell Biol* 10:19–29.
13. Luduena RF (1998) Multiple forms of tubulin: Different gene products and covalent modifications. *Int Rev Cytol* 178:207–275.
14. Westermann S, Weber K (2003) Post-translational modifications regulate microtubule function. *Nat Rev Mol Cell Biol* 4:938–947.
15. van Dijk J, et al. (2007) A targeted multienzyme mechanism for selective microtubule polyglutamylation. *Mol Cell* 26:437–448.
16. Verhey KJ, Gaertig J (2007) The Tubulin Code. *Cell Cycle* 6:2152–2160.
17. Campbell PK, et al. (2002) Mutation of a novel gene results in abnormal development of spermatid flagella, loss of intermale aggression and reduced body fat in mice. *Genetics* 162:307–320.
18. Ikegami K, et al. (2007) Loss of alpha-tubulin polyglutamylation in ROSA22 mice is associated with abnormal targeting of KIF1A and modulated synaptic function. *Proc Natl Acad Sci USA* 104:3213–3218.
19. Bonnet C, et al. (2001) Differential binding regulation of microtubule-associated proteins MAP1A, MAP1B, and MAP2 by tubulin polyglutamylation. *J Biol Chem* 276:12839–12848.
20. Boucher D, Larcher JC, Gros F, Denoulet P (1994) Polyglutamylation of tubulin as a progressive regulator of in vitro interactions between the microtubule-associated protein Tau and tubulin. *Biochemistry* 33:12471–12477.
21. Larcher JC, Boucher D, Lazereg S, Gros F, Denoulet P (1996) Interaction of kinesin motor domains with alpha- and beta-tubulin subunits at a tau-independent binding site. Regulation by polyglutamylation. *J Biol Chem* 271:22117–22124.
22. Janke C, et al. (2005) Tubulin polyglutamylase enzymes are members of the TTL domain protein family. *Science* 308:1758–1762.
23. Loebrich S, Bahring R, Katsuno T, Tsukita S, Kneussel M (2006) Activated radixin is essential for GABAA receptor alpha5 subunit anchoring at the actin cytoskeleton. *EMBO J* 25:987–999.
24. Dumoulin A, Levi S, Riveau B, Gasnier B, Triller A (2000) Formation of mixed glycine and GABAergic synapses in cultured spinal cord neurons. *Eur J Neurosci* 12:3883–3892.
25. Lappe-Siefke C, Maas C, Kneussel M (2008) Microinjection into cultured hippocampal neurons: A straightforward approach for controlled cellular delivery of nucleic acids, peptides and antibodies. *J Neurosci Methods* 175:88–95.
26. Brady ST, Pfister KK, Bloom GS (1990) A monoclonal antibody against kinesin inhibits both anterograde and retrograde fast axonal transport in squid axoplasm. *Proc Natl Acad Sci USA* 87:1061–1065.
27. Lippincott-Schwartz J, Cole NB, Marotta A, Conrad PA, Bloom GS (1995) Kinesin is the motor for microtubule-mediated Golgi-to-ER membrane traffic. *J Cell Biol* 128:293–306.
28. Kirsch J, Wolters I, Triller A, Betz H (1993) Gephyrin antisense oligonucleotides prevent glycine receptor clustering in spinal neurons. *Nature* 366:745–748.
29. Meyer G, Kirsch J, Betz H, Langosch D (1995) Identification of a gephyrin binding motif on the glycine receptor beta subunit. *Neuron* 15:563–572.
30. Hanus C, Vannier C, Triller A (2004) Intracellular association of glycine receptor with gephyrin increases its plasma membrane accumulation rate. *J Neurosci* 24:1119–1128.
31. Brugg B, Matus A (1991) Phosphorylation determines the binding of microtubule-associated protein 2 (MAP2) to microtubules in living cells. *J Cell Biol* 114:735–743.
32. Quinlan EM, Halpain S (1996) Postsynaptic mechanisms for bidirectional control of MAP2 phosphorylation by glutamate receptors. *Neuron* 16:357–368.
33. Lopez LA, Sheetz MP (1993) Steric inhibition of cytoplasmic dynein and kinesin motility by MAP2. *Cell Motil Cytoskeleton* 24:1–16.
34. von Massow A, Mandelkow EM, Mandelkow E (1989) Interaction between kinesin, microtubules, and microtubule-associated protein 2. *Cell Motil Cytoskeleton* 14:562–571.
35. Setou M, et al. (2002) Glutamate-receptor-interacting protein GRIP1 directly steers kinesin to dendrites. *Nature* 417:83–87.
36. Busciglio J, Lorenzo A, Yeh J, Yankner BA (1995) beta-amyloid fibrils induce tau phosphorylation and loss of microtubule binding. *Neuron* 14:879–888.
37. Fuhrmann JC, et al. (2002) Gephyrin interacts with Dynein light chains 1 and 2, components of motor protein complexes. *J Neurosci* 22:5393–5402.
38. Essrich C, Lorez M, Benson JA, Fritschy JM, Luscher B (1998) Postsynaptic clustering of major GABAA receptor subtypes requires the gamma 2 subunit and gephyrin. *Nat Neurosci* 1:563–571.